
First-Principles Calculations of Electronic Excitations in Clusters

LUCIA REINING,¹ OLIVIA PULCI,¹ MAURIZIA PALUMMO,²
GIOVANNI ONIDA²

¹Laboratoire des Solides Irradiés, CNRS-CEA, École Polytechnique, F-91128 Palaiseau, France

²Istituto Nazionale per la Fisica della Materia, Dipartimento di Fisica dell'Università di Roma "Tor Vergata", Via della Ricerca Scientifica, I-00133 Roma, Italy

Received 19 February 1999; accepted 1 September 1999

ABSTRACT: We discuss an approach to calculate electronic excitations in clusters, which starts from the determination of the ground state within density functional theory and the local density approximation, and subsequently yields electronic spectra from Green's function theory. These methods, which were originally developed and used in extended systems, are shown to work well also in clusters. We discuss the theory and the computational implementation, and illustrate the performance and the physical mechanisms of this approach for the example clusters Na₄, Na₆, and SiH₄. © 2000 John Wiley & Sons, Inc. *Int J Quant Chem* 77: 951–960, 2000

Key words: clusters; many-body effects; excitons; self-energy; electronic spectra

Introduction

The ground state properties of a wide class of realistic systems, including atomic and molecular aggregates, can be efficiently calculated from first principles using the density functional theory (DFT) [1] in the local density approximation (LDA) [1, 2]. This scheme yields generally very good results at a reasonable computational cost, as demonstrated by a very large number of studies of the structural and dynamical properties of clusters

published in the last two decades. However, the use of DFT-LDA as a theoretical tool for the study of physical properties other than the ground state, as in the calculation of electronic spectra (e.g., photoemission, inverse photoemission, or absorption), is not justified a priori since the Kohn–Sham eigenvalues cannot be directly interpreted as electron removal or addition energies, nor as the energies of neutral excitations. This problem can be overcome in part by working in the “delta self-consistent field” (Δ -SCF) scheme, which has been used for the calculation of ionization potentials. Also, in the more general case of photoemission spectra, where only the knowledge of one-particle excitations connected with the removal of an electron from a valence state is needed, a direct method based only

Correspondence to: L. Reining.

Contract grant sponsor: Italian Ministry of the University and Scientific Research (COFIN '97).

on DFT-LDA, albeit still approximated, has been recently devised by Ballone and Harris [3].

However, there is no general approach for the calculation of electronic spectra based only on the static DFT-LDA, in particular for absorption spectra. In fact, it is well known that the use of the DFT-LDA eigenvalues as the physical energies entering in the absorption process relies on several approximations. First of all, electron addition or removal energies (such as those measured in photoemission) should be obtained by using the true electron self-energy operator Σ , which appears instead of the DFT-LDA exchange-correlation potential in an equation similar to the Kohn–Sham equation. A good approximation for Σ , which allows determination of the quasiparticle (QP) band structure, can be obtained from Green’s functions theory within Hedin’s so-called GW approach [4]. In this scheme, DFT-LDA results can be used as the starting point in a first-order perturbative approach [5, 6]. The true QP energies, however, are in principle still not sufficient to correctly describe an absorption process in which electron–hole pairs are created. Their interaction can lead to a dramatic shift of peak positions as well as to appreciable distortions of the spectral line shape.

An alternative approach is that of the configuration interaction (CI) scheme, which is in principle able to yield the exact solution for ground as well as excited states: however, the computational cost of CI calculations grows in a prohibitive way with the system size (given the present computer capabilities, CI can hardly be used for systems with more than 10 electrons). Instead, using DFT-LDA results as a starting point for more refined calculations performed using Green’s function techniques allows the treatment of more complex systems, such as bulk semiconductors, surfaces, and clusters. This approach can be useful both for one-particle excitations (which can be computed within the GW method, yielding generally an excellent agreement with experimental results) or for two-particle excitations like those involved in the case of absorption, where an electron and a hole are created simultaneously [7–11].

Although the perturbative GW approach is now a well established and widely used technique for obtaining ab initio band structures in solids, the use of Green’s function techniques for first-principles calculations of spectral properties of clusters involving one- and two-particle excitations is still in its pioneering stage. However, the few existing works [10, 11] have yielded promising results. Hence, it is

worthwhile to make an effort to report a comprehensive overview of the basic theoretical ingredients and the particular computational implementation for calculations done in a standard plane wave basis, and to investigate the physical effects that dominate the spectral features, by considering some computationally relatively simple systems, namely, small alkaline and hydrogenated silicon clusters. We discuss in particular Na_4 , for which a part of the results (i.e., the absorption spectrum) has already been published previously [10]. We have repeated those calculations with improved precision, which leads in fact to better agreement with experiment. Moreover, we discuss in detail the GW corrections and the resulting agreement with experimental ionization potentials for Na_4 , Na_6 , and SiH_4 .

Theory

In this section, we introduce the one-particle Green’s function and the exchange-correlation self-energy as the relevant quantities for a description of one-particle excitations. We give a short overview of the relevant Green’s functions equations [4], which shows how the so-called GW approximation for the self-energy is obtained from an iteration process. Next, we discuss the two-particle Green’s function, which governs processes containing electron–hole excitations, like in optical absorption. We point out the most important approximations that are made in the independent-GW quasiparticle approach when constructing an optical spectrum. We introduce the Bethe–Salpeter equation, which describes excitonic effects, as a continuation of the iteration process beyond GW, and show how the equation can be transformed to an effective eigenvalue problem that is physically intuitive and allows for a detailed analysis of the excitonic effects [12].

We start from the DFT-LDA Kohn–Sham (KS) equation

$$\hat{h}_{\text{KS}}^{\text{eff}}\varphi_i = \left[-\frac{1}{2}\nabla^2 + \hat{v}_{\text{eff}}\right]\varphi_i = \epsilon_i\varphi_i, \quad (1)$$

with

$$v_{\text{eff}}(\mathbf{r}) \equiv v_{\text{ext}}(\mathbf{r}) + \int d\mathbf{r}' \frac{n(\mathbf{r}')}{|\mathbf{r} - \mathbf{r}'|} + V_{\text{xc}}(\mathbf{r}), \quad (2)$$

$$V_{\text{xc}}(\mathbf{r}) \equiv \frac{\delta}{\delta n(\mathbf{r})} E_{\text{xc}}[n], \quad (3)$$

which is generally used to determine ground-state total energies and related quantities via the resulting charge density $n(\mathbf{r}) = \sum_i^{\text{occ}} |\varphi_i(\mathbf{r})|^2$. However, often not only ground-state properties are derived from

the KS equation, but also the resulting eigenvalues ϵ_i and eigenfunctions φ_i are used as physical quantities. In particular, the eigenvalues are interpreted as electron addition and removal energies. This can give reasonable results, in particular for the occupied bands of standard semiconductors and insulators. It is, however, well known that the true electron addition and removal energies are of a much more complicated nature, and that the KS approach in particular fails to describe the gap between occupied and empty states. A correct description of such quantities, given by one-quasiparticle excitations, can be obtained from Green's function theory. In particular, quasiparticle energies are given by the energy poles of the one-particle Green's function, which can in principle be obtained from Hedin's set of coupled equations [4] involving the Hartree Hamiltonian H_0 , the one-particle Green's function G (which describes the propagation of an electron or hole in the system), the self-energy Σ (containing the exchange-correlation potential acting on a quasiparticle in some excited state), the polarizability function P (which expresses the response of the system to the total potential), the bare Coulomb interaction v , the screened (effective) Coulomb interaction W , and finally the vertex function Γ :

$$(\omega - H_0(\mathbf{x}))G(\mathbf{x}, \mathbf{x}', \omega) - \int d\mathbf{x}'' \Sigma(\mathbf{x}, \mathbf{x}'', \omega)G(\mathbf{x}'', \mathbf{x}', \omega) = \delta(\mathbf{x}, \mathbf{x}'), \quad (4)$$

$$\Sigma(12) = i \int d(34)W(1^+3)G(14)\Gamma(42; 3), \quad (5)$$

$$W(12) = v(12) + \int d(34)W(13)P(34)v(42), \quad (6)$$

$$P(12) = -i \int d(34)G(23)G(42)\Gamma(34; 1), \quad (7)$$

$$\Gamma(12; 3) = \delta(12)\delta(13) + \int d(4567) \frac{\delta \Sigma(12)}{\delta G(45)} \times G(46)G(75)\Gamma(67; 3). \quad (8)$$

The argument (l) is used to indicate (\mathbf{x}_l, t_l) . These equations implicitly define the (otherwise unknown) self-energy, but cannot be solved exactly. Note that the neglect of Σ yields the Hartree theory, and its substitution with the DFT exchange-correlation potential V_{xc} would lead back to the KS equations. To obtain a better approximation for the self-energy, Hedin proposed an iteration of the equations starting from a bare vertex, i.e., $\Gamma = \delta$ in Eq. (8). Equation (7) becomes then simply

$$P(12) = -iG(21)G(12), \quad (9)$$

i.e., the independent particle, or RPA, polarizability. Considering this approximation can help to clarify the role of the vertex function Γ : when using a bare vertex, the response of the system to a perturbation is given in terms of the creation of electron-hole pairs, GG , which do not interact. Dressing the vertex beyond $\Gamma = \delta$ allows for electron-hole interaction. W is then constructed from P , and Σ is obtained as

$$\Sigma(12) = iG(12)W(1^+2), \quad (10)$$

which is the well known GW approximation. Usually, Eq. (4) is transformed to the eigenvalue equation

$$H_0(\mathbf{x})\psi_s(\mathbf{x}) + \int d\mathbf{x}' \Sigma(\mathbf{x}, \mathbf{x}'; E_s)\psi_s(\mathbf{x}') = E_s\psi_s(\mathbf{x}), \quad (11)$$

which results from the spectral representation of the Green's function

$$G(\mathbf{x}, \mathbf{x}'; \omega) = \sum_s \psi_s(\mathbf{x}; \omega)\psi_s^*(\mathbf{x}'; \omega)/(\omega - E_s(\omega))$$

and from the fact that well-defined quasiparticles are occurring at sharp poles of the Green's function, i.e., at $\omega = E_s(\omega)$.

In a practical application, Eq. (11) is built up by constructing the starting-point Green's function G , and hence W and Σ , from LDA eigenfunctions and eigenvalues. Using the close resemblance of Eqs. (1) and (11), it is then solved to first order in the difference between Σ and the LDA exchange-correlation potential V_{xc} . Quasiparticle energies E_s in excellent agreement with experiments such as photoemission and inverse photoemission spectroscopy have been obtained in such a way for a broad range of extended systems and for a few finite systems.

To obtain an absorption spectrum, we have to work with the dielectric matrix ϵ , which is linked to the screened Coulomb interaction W by $W = \epsilon^{-1}v$. In fact, absorption is given by the macroscopic dielectric constant

$$\epsilon_M(\omega) = \lim_{\mathbf{q} \rightarrow 0} \frac{1}{\epsilon_{G=0, G'=0}^{-1}(\mathbf{q}; \omega)}. \quad (12)$$

The most straightforward way to deal with this problem is (a) to use the same RPA polarizability (9) used for the GW calculation, i.e., constructed using LDA energies, and (b) to approximate $\lim_{\mathbf{q} \rightarrow 0} (1/\epsilon_{G=0, G'=0}^{-1}(\mathbf{q}; \omega))$ by $\lim_{\mathbf{q} \rightarrow 0} \epsilon_{G=0, G'=0}(\mathbf{q}; \omega)$, which means to neglect local field effects. This approach yields the standard formula for optical absorption,

$$\text{Im}(\epsilon_M(\omega)) = \text{Im} \left(\lim_{\mathbf{q} \rightarrow 0} v(\mathbf{q}) \sum_{v,c} \frac{|\langle v|e^{i\mathbf{q}\mathbf{r}}|c\rangle|^2}{(E_c - E_v - \omega - i\eta)} \right), \quad (13)$$

where v and c are filled and empty LDA states, respectively. We call this LDA-RPA for the illustrations in the Results section. The resulting spectra can often explain qualitative features, but are generally not satisfactory, as will be seen later. Much work has been done for some years to go beyond approximations (a) and (b). On one hand, approximation (a) has been weakened by substituting GW quasiparticle energies for the LDA energies in the construction of the Green's function, while maintaining the RPA form $P = -iGG$. In some cases, this can lead to significant improvements in the resulting spectra, but we will show that this is not at all the case for small clusters. We will call this approach the GW-RPA. On the other hand, the inversion of ϵ has been carried out to include local-field effects and avoid approximation (b). This can also yield improvements in some energy ranges. However, still quite often the calculated absorption spectra are in striking disagreement with experiment.

In fact, just using the GW eigenvalues in the construction of P is not sufficient—we have to construct P from a true second iteration of Eqs. (4)–(8). This means we have to go again through Eq. (8), now using $\Sigma = iGW$, and not just update eigenvalues in (9), i.e., in (13). Doing so yields an integral equation for Γ :

$$\Gamma(12;3) = \delta(12)\delta(13) + i \int d(67)W_0(1^+2)G(16)G(72)\Gamma(67;3) \quad (14)$$

[here we have used $\delta\Sigma/\delta G = iW_0$, neglecting the small term $iG(\delta W_0/\delta G)$; W_0 is the W used in Σ , i.e., based on the RPA polarizability P_0 of (9)]. We can transform (14) to an integral equation for a generalized \hat{P} by multiplying with $-iG(41)G(25)$ and integrating over $d(12)$,

$$\hat{P}(3;45) = -iG(43)G(35) + i \int d(12)\hat{P}(3;12)W_0(1^+2)G(41)G(25), \quad (15)$$

and then use that $P(35) = \hat{P}(3;55)$. This equation has to be used together with

$$\epsilon(12) = \delta(12) - \int d(3)P(32)v(13), \quad (16)$$

which results from (6), and Eq. (12) for the macroscopic dielectric constant. The result can be written as a Bethe–Salpeter equation [14]

$$S(1,1';2,2') = S_0(1,1';2,2') + S_0(1,1';3,3')\Xi(3,3';4,4')S(4,4';2,2'), \quad (17)$$

where

$$\epsilon_M(\omega) = 1 - \lim_{\mathbf{q} \rightarrow 0} v(\mathbf{q})\hat{\chi}_{\mathbf{G}=0, \mathbf{G}'=0}(\mathbf{q};\omega) \quad (18)$$

and $\hat{\chi}(\mathbf{r}, \mathbf{r}'; \omega) = -iS(\mathbf{r}, \mathbf{r}, \mathbf{r}', \mathbf{r}'; \omega)$.

We integrate over repeated arguments. The term $S_0(1,1';2,2') = G(1',2')G(2,1)$ yields the polarization function of independent quasiparticles χ_0 , from which the standard RPA ϵ_M , neglecting local field effects, is obtained. The kernel Ξ contains two contributions:

$$\Xi(1,1',2,2') = -i\delta(1,1')\delta(2,2')v(1,2) + i\delta(1,2)\delta(1',2')W_0(1,1'). \quad (19)$$

Considering the first term in the calculation of S is equivalent to including local-field effects in the matrix inversion of a standard RPA calculation. When spin is not explicitly treated, v gets a factor of 2 for singlet excitons. In the second term, W_0 is the screened Coulomb attraction between electron and hole. We limit ourselves to static screening, since dynamical effects in the electron–hole screening and in the one-particle Green's function tend to cancel each other [13], which suggests neglecting both of them.

To solve Eq. (17), we have to invert a four-point function. In Ref. [14] this was possible due to the use of a very limited basis set. In an ab initio plane wave calculation, such a procedure is clearly prohibitive when plane waves are chosen as straightforward basis functions. This is particularly true for clusters, where the necessity to use a large unit cell to avoid interactions with the artificial periodic images leads to a huge number of plane waves. Instead, the physical picture of interacting electron–hole pairs suggests using a basis of LDA eigenfunctions, $\varphi_n(\mathbf{r})$, expecting that only a limited number of electron–hole pairs will contribute to each excitation. In fact, for the case of small clusters treated here it turns out that the choice of a plane wave basis leads to matrix sizes on the order of $10^6 \times 10^6$, whereas matrices smaller than $10^3 \times 10^3$ have to be treated with the present choice.

In this basis, $\chi_0^{(n_1, n_2), (n_3, n_4)} = \delta_{n_1, n_3} \delta_{n_2, n_4} (f_{n_2} - f_{n_1}) / (E_{n_2} - E_{n_1} - \omega)$ and, after solving for S , in the case of static screening, Eq. (17) can be written as

$$S_{(n_1, n_2), (n_3, n_4)} = (H_{\text{exc}} - I\omega)_{(n_1, n_2), (n_3, n_4)}^{-1} (f_{n_4} - f_{n_3}), \quad (20)$$

with

$$H_{\text{exc}}^{(n_1, n_2), (n_3, n_4)} = (E_{n_2} - E_{n_1})\delta_{n_1, n_3} \delta_{n_2, n_4} - i(f_{n_2} - f_{n_1}) \times \int d\mathbf{r}_1 \int d\mathbf{r}'_1 \int d\mathbf{r}_2 \int d\mathbf{r}'_2 \psi_{n_1}(\mathbf{r}_1) \psi_{n_2}^*(\mathbf{r}'_1) \times \Xi(\mathbf{r}_1, \mathbf{r}'_1, \mathbf{r}_2, \mathbf{r}'_2) \psi_{n_3}^*(\mathbf{r}_2) \psi_{n_4}(\mathbf{r}'_2). \quad (21)$$

I is the identity operator. The energies E_n are the QP levels. Together with the above form of χ_0 , this is consistent with the use of LDA wave functions and updated energy denominators in the Green's function after the first iteration of Eqs. (4)–(8), i.e., after the GW calculation. The f_n are Fermi–Dirac occupation numbers. We further retain only the so-called resonant part of this Hamiltonian, i.e., those contributions where n_1 stands for an occupied state and n_2 stands for an empty state, which turns out to be an excellent approximation (for a discussion of the general case, see Ref. [12]). We avoid inverting the matrix $(H_{\text{exc}} - I\omega)$ for each absorption frequency ω by applying the identity

$$(H_{\text{exc}} - I\omega)^{-1} = \sum_{\lambda} \frac{|\lambda\rangle\langle\lambda|}{(E_{\lambda} - \omega)}, \quad (22)$$

which holds for a system of eigenvectors and eigenvalues of a Hermitian matrix defined by

$$H_{\text{exc}}|\lambda\rangle = E_{\lambda}|\lambda\rangle. \quad (23)$$

Equation (23) is the effective two-particle Schrödinger equation, which we solve by diagonalization. Explicit knowledge of the coupling of the various two-particle channels, given by the coefficients $A_{\lambda}^{(n_1, n_2)}$ of the state $|\lambda\rangle$ in our LDA basis, allows us to identify the character of each transition.

The macroscopic dielectric function in Eq. (18) is obtained as

$$\epsilon_M(\omega) = 1 + \left(\lim_{q \rightarrow 0} v(\mathbf{q}) \sum_{\lambda} \frac{|\sum_{v,c} \langle v|e^{-i\mathbf{q}\mathbf{r}}|c\rangle A_{\lambda}^{(v,c)}|^2}{(E_{\lambda} - \omega)} \right). \quad (24)$$

In practice, the KS eigenvalues and eigenfunctions from a DFT-LDA calculation serve as input to the evaluation of the RPA screened Coulomb interaction W and the GW self-energy Σ . The KS eigenfunctions, together with the QP energies and W , are then used in the exciton calculation.

Equations (23) and (24) constitute a set of equations that have been frequently used in frameworks that are not ab initio [15, 16]. Here, it appears as a particular approximation to the more general formula (21), with well-defined ab initio ingredients that are consistent with the GW approach.

Technical Details

The first step in calculating the absorption spectra and the photothresholds of the clusters is the determination of the geometrical structures. These have been determined within the DFT-LDA scheme

by using a Car–Parrinello approach [17]. All technical details are as given in Ref. [10]. In particular, we have used an energy cutoff of 6 Ry and norm-conserving pseudopotentials including nonlinear core corrections [18]. An important parameter of the calculations is the size of the supercell used to describe an isolated cluster: the supercell must be large enough (that is, must have enough empty space) to guarantee that near cluster images do not interact, but also be small enough to render the computational effort feasible. The convergence behavior of the LDA eigenvalues and equilibrium geometries has been carefully tested. We have found that the relative positions of the eigenvalues, and in particular the highest occupied molecular orbital–lowest unoccupied molecular orbital (HOMO–LUMO) gap, converge to better than 10 meV using a supercell of 36 au for the neutral Na₄ cluster, and at 42 au for the neutral Na₆ cluster. For the relaxation of charged clusters, we add a homogeneous charged background to avoid divergencies. We therefore need a bigger supercell, typically of 65 au, to have reliable geometries. The absolute values of the eigenvalues, however, converge more slowly with the cell size; since the absolute position of the last occupied eigenstate plays a fundamental role in the determination of the photothresholds, we decided to perform our LDA calculations using a supercell of 80 au for all sodium clusters so that the eigenvalue positions with respect to the vacuum level converge within 10 meV. In the GW calculation, instead, we could restrict ourselves to a cell of 36 au for Na₄ and 42 au for Na₆. These choices yield sufficiently converged results thanks to the introduction of a cutoff of the long-range part of the Coulomb interaction, which was proposed in Ref. [10]. In fact, as was pointed out in that work, a straightforward GW calculation would converge only at huge cell sizes, since a charged system (i.e., a cluster with an additional electron or hole) is described. The proposed cutoff is applied by simply suppressing the long-range tail of the Coulomb interaction beyond a distance c , which must be larger than the diameter of a sphere circumscribing the charge density of the cluster, and smaller than half the distance to the nearest-neighbor cluster. We have checked that in this way our GW corrections for the states around the Fermi level converge with an error of less than 30 meV for the given cell sizes. The same choices as in the GW calculation are then made for the subsequent calculation of the optical spectrum.

For the calculations on SiH₄, we used norm-conserving pseudopotentials [19], with a plane-wave cutoff of 20 Ry and supercells of 30 and 40 au to check convergence. The error bar for the absolute position of the occupied levels in this case is 0.15 eV, since we did not perform this calculation at 80 au, as in the case of the sodium clusters. The converged result can be extrapolated to be about 0.1 eV lower than the values given here. However, due to the order of magnitude of the effects calculated here, this obviously does not influence the conclusions.

Results

ELECTRON ADDITION AND REMOVAL ENERGIES

In principle, the eigenvalues of Eq. (11) could be directly compared to experimental photoemission results. In particular, the energy of the highest occupied level should correspond to the ionization potential. However, due to the small number of valence electrons contained in clusters built up of few atoms, we can expect that their geometrical structure can be strongly modified when an electron is added or removed from the system. In fact, as in the case of molecules, both an adiabatic and a vertical ionization potential can be defined, differing by an energy amount corresponding to this structural relaxation. Moreover, even the *symmetry* of the relaxed and unrelaxed structure can be different, producing very interesting and evident effects (e.g., by changing the number of peaks in the photoemission spectrum).

To include these effects in the theoretical spectra, we should hence calculate the relaxation (or Jahn-Teller) energy, and combine it with the “vertical” addition or removal energies computed within the GW scheme. A method to solve this problem has been illustrated by some of us, taking silane as an example [20].

We first observe that the photoemission spectrum is determined by the energy difference between the starting (N electron) cluster, which we suppose to be neutral, and the $N - 1$ electron system in a distorted geometrical configuration:

$$E^p = E_0^N - E_{\text{dist}}^{N-1}. \quad (25)$$

Hence the GW removal energies, which in fact represent the quantity $E^{\text{GW}} = E_{\text{geo}}^N - E_{\text{geo}}^{N-1}$ computed in either geometry and labeled by geo, are not sufficient to determine the relevant energy difference.

However, the latter can be rewritten by adding and subtracting the total energy of the N -electron cluster in the *distorted* configuration,

$$E^p = E_0^N + E_{\text{dist}}^N - E_{\text{dist}}^N - E_{\text{dist}}^{N-1} = \Delta_E^N + \epsilon_{\text{dist}}^{\text{GW}}, \quad (26)$$

where Δ_E^N is the energy difference for the ground state of the N -electron cluster in two different geometries, a quantity that can be easily evaluated within DFT-LDA, and $\epsilon_{\text{dist}}^{\text{GW}}$ is the GW “vertical” removal energy computed for the distorted cluster at fixed geometry.

We have applied this scheme to Na₄, Na₆, and SiH₄, and a discussion of the results follows.

Na₄

The Na₄ equilibrium structure turns out to be a planar rhombus, in agreement with a variety of results from different calculations [10, 21, 22]. We obtain a distance between atoms of 5.73 au on the short and 11.71 au on the long axis of the cluster, which is about 5% more than the distances obtained in Ref. [21]. This is consistent with the fact that in Ref. [21] nonlinear core corrections have not been used. When a hole is created in the HOMO, Na₄ still remains a planar rhombus, but with a short axis of 6.02 au and a long axis of 11.97 au. The bond angles change very slightly from the neutral cluster to the configuration with one hole: the values are 52 and 128° and 53 and 127°, respectively. We again find similar agreement with previous calculations, [21] as for the case of the neutral cluster.

The ionization potential calculated by simply using the LDA eigenvalue of the HOMO is 2.76 eV, in striking disagreement with the experimental result [23] of 4.27 ± 0.05 eV. Simply adding our calculated GW correction in the neutral geometry, which is a downward shift of 1.53 eV, yields the vertical ionization potential of 4.29 eV. Instead, going through the procedure described above so as to include geometrical relaxations yields an adiabatic ionization potential of 4.27 eV, in excellent agreement with experiment. To be precise, we should stress the fact the tiny difference between the two theoretical results essentially stems from the relaxation energy $E_0^N - E_{\text{dist}}^N$. Its magnitude is within the precision of our GW calculations, and we can hence not distinguish between the vertical and the adiabatic ionization potentials of Na₄. In fact, the authors of [23] find that the difference between the vertical and the adiabatic ionization potentials is within the experimental error bar of 50 meV.

By way of contrast, our result is in better agreement with experiment than the Δ -SCF result of Martins et al. [21], which, from Figure 6 of that reference, turns out to be about 4.4 eV. They are also very much improved with respect to the results of an approximate GW calculation on a jellium sphere representing the Na₄ cluster [24].

Na₆

We find that the geometry of Na₆ in its neutral state is a relatively flat pentagonal pyramid of slightly broken C_{5v} symmetry. This agrees with the findings of other authors [21, 25, 26]. Our calculated bond lengths are slightly shorter than those of the CI calculation of Ref. [22] and about 6% longer than those of Ref. [21].

Na₆⁺ can be obtained from Na₆ through a relatively strong distortion. We can again compare our results to those of Ref. [21] and find a similar explainable discrepancy as for the results on the other clusters. It should be noted that the geometries of these clusters present several local minima lying energetically relatively close to the equilibrium structure, which makes it difficult to give definite answers concerning the geometries that might appear in the real experimental situation.

The LDA eigenvalue of the HOMO calculated in the geometry of the neutral cluster turns out to be again more than 1 eV smaller in absolute value than the experimental ionization potential. The total vertical ionization potential, including the GW correction, turns out to be 4.45 eV. Instead, in the distorted geometry we find an LDA eigenvalue of -2.62 eV, to which the GW correction of -1.37 eV has to be added. Here, in contrast to Na₄, the geometrical relaxation energy $E_0^N - E_{\text{dist}}^N$ is appreciable, namely, -0.3 eV. Moreover, since the distortion of the cluster lowers its symmetry, the double degeneracy of the HOMO is now split into two levels. The second level has an LDA eigenvalue of -3.28 eV in the distorted geometry, and a GW correction of -1.40 eV. An additional broadening of 0.7 eV has hence to be added to the first peak of the photoionization spectrum. From the highest occupied eigenvalue, we obtain a total adiabatic ionization potential of 4.29 eV, which is hence close to the Δ -SCF result of Martins et al. [21] and only slightly overestimated with respect to the experimental value of 4.12 ± 0.05 eV [23]. It should be noted that Herrmann et al. [23] claimed that vertical and adiabatic potentials are indistinguishable with the energy resolution obtainable in their experiment. Since we

find a difference of 0.16 eV between our calculated vertical and adiabatic ionization potentials (significant differences have also been reported in [21]), and since, as pointed out above, the peak is broadened due to the symmetry lowering, it is not clear whether the theoretical and experimental results really can be compared with an error bar of 50 meV on both sides.

SiH₄

To show the case of a system where geometry effects are very important, we also report calculations on SiH₄ [20].

SiH₄ in its neutral state possesses the full T_d symmetry, i.e., a silicon atom sitting at the center of a cube, with the hydrogen atoms situated on four of the cube corners. The Si—H bond length is 2.87 au in good agreement with results of other authors [27]. The ionized cluster undergoes a Jahn–Teller distortion to a system with D_2 symmetry, with a bond length of 2.93 au and H—Si—H angles of 98 and 136°. The highest occupied LDA eigenvalue in the ideal geometry is triply degenerate and situated at -8.2 eV. Experimentally, a broad peak at 11.5–13.5 eV has been reported [28] in the photoemission spectrum of SiH₄. Again, the LDA value dramatically underestimate the ionization potential. The Jahn–Teller distortion splits the HOMO and gives a single level at -6.99 eV and a doubly degenerate one at -8.59 eV, still far off the experimental values. The GW corrections, comparable to what has been reported in [11], shift these values to -11.99 and -10.49 eV, respectively. A strong improvement has hence been obtained, but still the difference with the experimental values is significant. Finally we add the difference in total energy Δ_E^N of the neutral cluster in the two geometries, which turns out to be as large as -0.74 eV. The resulting values of -11.23 and -12.73 eV compare well with the experimental findings.

ABSORPTION: Na₄

Important experimental information on small clusters is often obtained from photoionization experiments as well as from approaches involving the absorption of photons. One typical example is photodepletion, which leads to a spectrum that is under certain conditions (see, e.g., [29]), directly comparable to an absorption spectrum. The calculation of such a spectrum in a small cluster leads to dramatic discrepancies with experiment when an

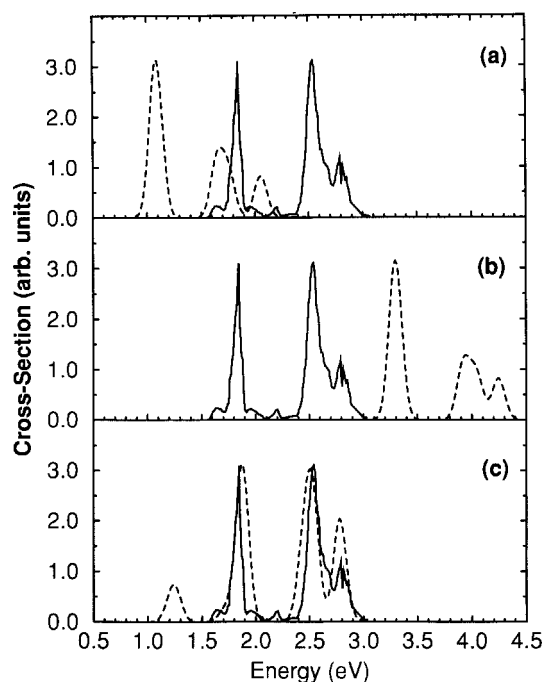


FIGURE 1. Computed first-principle absorption spectrum of Na_4 (dashed line) compared with experimental photodepletion cross sections obtained from Ref. [29] (solid line). (a) LDA-RPA result; (b) GW-RPA calculation; (c) result obtained including excitonic effects.

independent-particle approach is applied, but can be enormously improved by the inclusion of the electron-hole interaction, as will be shown in the following example.

The continuous lines in Figure 1(a)–(c) show the experimental photodepletion spectrum of Wang et al. [29]. The dashed line in panel (a) is our LDA-RPA result, which is hence obtained by evaluating Eq. (13) using LDA eigenvalues and eigenfunctions. Neither the peak positions nor the relative intensities are in satisfactory agreement with experiment. (Note that the absolute intensities of the calculated and the experimental spectrum cannot be compared. We have hence aligned the height of the theoretical peak of lowest energy to the experimental peak. The spectra are shown in the energy range corresponding to a range up to 3 eV in the experimental spectrum, since our results are well converged up to that energy.) One could now hope to improve the spectrum by substituting the physical quasiparticle energies obtained via the GW corrections for the LDA-KS eigenvalues. It is reasonable to leave the wave functions unchanged, since it has been shown that in general LDA and quasiparticle wave

functions closely match each other. This GW-RPA result is given by the dashed line in panel (b). It is obvious that no improvement is obtained concerning the intensities: as in solids, the GW correction yields essentially a rigid shift of the spectrum. More important, the spectrum is dramatically displaced to higher energies, leading to an overestimation of more than 1.5 eV of the position of the first main peak.

The dashed curve in panel (c) finally shows the result that is obtained, including the electron-hole interaction via the solution of Eqs. (23) and (24). Such a spectrum was already published in [10]. We have performed the calculations again, and the present theoretical result is even slightly improved. The reason for this change is a more precise determination of the quasiparticle energies of high-lying empty states (starting from about 4 eV above the HOMO), which have turned out to influence the absorption spectrum in a nonnegligible way. The final result in Figure 1 shows excellent agreement with experiment, both for the peak positions and for relative intensities.

As pointed out in Ref. [10], the reason for the very strong electron-hole interaction in small clusters is the low effective screening due to the finite size of the cluster. This leads to two major effects: First, already a first-order perturbation ansatz for the solution of Eq. (21) with respect to the independent-quasiparticle result would yield strong shifts of the absorption peaks, which is not true in a solid. Second, although the single-particle states, and hence transition energies, in such small clusters are well spaced, different transitions interact strongly via the still important off-diagonal elements of the exciton Hamiltonian, which leads to state mixing and hence strong redistributions of oscillator strength. We have been able to compare our analysis for the contributions to the main peaks with the CI results, and found similar results [10].

Discussion of Electron Addition and Removal Energies

In view of the very important GW corrections which we find in these small clusters (note that the HOMO-LUMO gap in Na_4 is multiplied by more than a factor of 5 when going from the LDA to GW), it is worthwhile to study the different contributions in a bit more detail. In fact, for the sodium clusters we find a strong downward shift of all occupied states, of the order of 1.5 eV, which is dominated

by the contribution of the bare exchange term: this term amounts to about -5 eV, whereas the correlation contribution is of the order of -1 eV. The strong shift should hence be related to the localization of the occupied states. The empty states shift upward, with corrections starting from contributions around 0.9 eV for the LUMO and smoothly vanishing when going to high energies where the states become plane-wave-like. For the unoccupied states, the bare exchange and the correlation contributions are of similar magnitude. Both occupied and low-lying unoccupied states show a relatively strong renormalization factor due to dynamical effects, i.e., due to the fact that the self-energy depends (almost linearly) on the energy, which introduces the necessity to solve Eq. (11) self-consistently or, as we do it, by linearization of Σ in energy. In standard semiconductors, this renormalization reduces the GW corrections by typically a factor of 0.78 for silicon to 0.87 for lithium chloride. For our sodium clusters, this can be lowered up to a factor of 0.70 , which indicates that it might be worthwhile to investigate possible effects beyond the GW approximation on these systems.

It is very interesting to compare these findings on the sodium clusters to the behavior that we find for SiH_4 . Also in SiH_4 , screening is low due to the finite cluster size, but it is moreover lowered due to the fact that the cluster is built up of atoms which are less polarizable than the sodium atoms. As a consequence, we have now a bare exchange contribution of almost -15 eV to the self-energy matrix elements for occupied states, whereas the correlation contribution is as small as 0.4 eV and is positive. This change in sign indicates that it is dominated by the screening of the exchange term, and not by the Coulomb hole, which is due to the adiabatic build-up of the screening of the hole. Also dynamical effects, as expressed by the renormalization factor, are very small: this factor is now merely 0.88 , instead of 0.7 for the sodium clusters. SiH_4 could hence probably be efficiently described by a self-interaction correction to the LDA result and, on the other hand, would not be a good candidate for an investigation of the effects of corrections beyond the GW approximation.

Conclusion

In conclusion, for the example of three small clusters we have illustrated how different many-body effects can be included in the calculation of spectroscopic properties of clusters beyond the standard DFT Kohn–Sham approach.

We have discussed the underlying theory and shown how self-energy corrections in the GW approach improve results of photoionization and how excitonic effects contribute to absorption spectra. The application of these type of approaches, borrowed from solid state physics, seems hence to be promising even for the physics of clusters, and it will be worthwhile to investigate the origin of the remaining discrepancies with experiment, which may be searched in the cluster geometries, technical details, or even the need to go beyond the present level of theory.

Note Added in Proof

Promising results for the absorption spectra of small sodium clusters have recently also been obtained by calculations based on time dependent DFT (TDDFT) [Vasiliev, I.; Ögüt, S.; Chelikowsky, J. *Phys Rev Lett* 1999, 82, 1919].

ACKNOWLEDGMENTS

For this project, computer time on the Cray C98 was granted by IDRIS (Project No. CP9/990544). We thank S. Goedecker for providing us efficient code for fast Fourier transforms [30]. We are also indebted to the Italian Ministry of the University and Scientific Research (MURST) for financial support (COFIN '97).

References

- Hohenberg, P.; Kohn, W. *Phys Rev* 1964, 136, B864. Kohn, W.; Sham, L. *Phys Rev* 1965, 140, A1133.
- Ceperley, D. M.; Alder, B. J. *Phys Rev Lett* 1980, 45, 566. Perdew, J. P.; Zunger, A. *Phys Rev B* 1981, 23, 5048.
- Ballone, P.; Harris, J. *Chem Phys Lett* 1999, 303, 420.
- Hedin, L. *Phys Rev A* 1965, 139, 796.
- Hybertsen, M. S.; Louie, S. G. *Phys Rev Lett* 1985, 55, 1418; *Phys Rev B* 1986, 34, 5390.
- Godby, R. W.; Schlüter, M.; Sham, L. J. *Phys Rev Lett* 1986, 56, 2415; *Phys Rev B* 1988, 37, 10159.
- Albrecht, S.; Reining, L.; Del Sole, R.; Onida, G. *Phys Rev Lett* 1998, 80, 4510.
- Benedict, L.; Shirley, E.; Bohn, R. *Phys Rev B* 1998, 57, R9385; *Phys Rev Lett* 1998, 80, 4515.
- Rohlfing, M.; Louie, S. *Phys Rev Lett* 1998, 81, 2312.
- Onida, G.; Reining, L.; Godby, R. W.; Del Sole, R.; Andreoni, W. *Phys Rev Lett* 1995, 75, 818.
- Rohlfing, M.; Louie, S. *Phys Rev Lett* 1998, 80, 3320; *Phys Rev Lett* 1999, 82, 1959.

12. Albrecht, S.; Reining, L.; Del Sole, R.; Onida, G. *Phys Status Solidi A* 1998, 170, 189.
13. Bechstedt, F.; Tenelsen, K.; Adolph, B.; Del Sole, R. *Phys Rev Lett* 1997, 78, 1528.
14. Hanke, W.; Sham, L. J. *Phys Rev Lett* 1979, 43, 387; *Phys Rev B* 1980, 21, 4656.
15. Strinati, G. *Phys Rev Lett* 1982, 49, 1519; *Phys Rev B* 1984, 29, 5718.
16. Bassani, F.; Pastori Parravicini, G. *Electronic States and Optical Transitions in Solids*; Pergamon: Oxford, 1975; Chapter 6.
17. Car, R.; Parrinello, M. *Phys Rev Lett* 1985, 55, 2471.
18. Giannozzi, P. Unpublished.
19. Bachelet, G.; Hamann, D. R.; Schlüter, M. *Phys Rev B* 1982, 26, 4199. Troullier, N.; Martins, J. *Phys Rev B* 1991, 43, 1993.
20. Reining, L.; Onida, G.; Albrecht, S. *Comp Math Sci* 1998, 10, 444.
21. Martins, J. L.; Buttet, J.; Car, R. *Phys Rev B* 1985, 31, 1804.
22. Bonacic-Koutecky, V.; Fantucci, P.; Koutecky, J. *J Chem Phys* 1990, 93, 3802; *Chem Phys Lett* 1990, 166, 32.
23. Herrmann, A.; Schumacher, E.; Woeste, L. *J Chem Phys* 1978, 68, 2327.
24. Saito, S.; Zhang, S. B.; Louie, S. G.; Cohen, M. L. *Phys Rev B* 1989, 40, 3643.
25. Röthlisberger, U.; Andreoni, W. *J Chem Phys* 1991, 94, 8129.
26. Bonacic-Koutecky, V.; Pitter, J.; Sheush, C.; Guest, M. F.; Koutecky, J. *J Chem Phys* 1992, 96, 7938.
27. Onida, G.; Andreoni, W. *Chem Phys Lett* 1995, 243, 183.
28. Feher, F. *Molekuelnspektroskopische Untersuchungen auf dem Gebiet der Silane und der Heterocyclischen Sulfane*, Forschungsbericht des Landes Nordrhein-Westfalen; Westdeutscher Verlag: Köln, 1977.
29. Wang, C. R. C.; Pollack, S.; Cameron, D.; Kappes, M. M. *J Chem Phys* 1990, 93(6).
30. Goedecker, S. *Comp Phys Commun* 1993, 76, 294; *SIAM J Sci Comput* 1997, 18, 1605.